Expansion on matrix deposited by nonchondrogenic urine stem cells strengthens repeated passage bone marrow stromal cells' chondrogenic capacity

Ming Pei,

Stem Cell and Tissue Engineering Laboratory, Department of Orthopaedics, West Virginia University, Morgantown, WV 26506 USA. Exercise Physiology, West Virginia University, Morgantown, WV 26506 USA. Mechanical & Aerospace Engineering, West Virginia University, Morgantown, WV 26506 USA

Jingting Li,

Stem Cell and Tissue Engineering Laboratory, Department of Orthopaedics, West Virginia University, Morgantown, WV 26506 USA. Exercise Physiology, West Virginia University, Morgantown, WV 26506 USA

Ying Zhang,

Stem Cell and Tissue Engineering Laboratory, Department of Orthopaedics, West Virginia University, Morgantown, WV 26506 USA. Mechanical & Aerospace Engineering, West Virginia University, Morgantown, WV 26506 USA

Guihua Liu,

Wake Forest Institute for Regenerative Medicine, Winston-Salem, NC 27157 USA

Lei Wei, and

Molecular Biology Laboratory, Department of Orthopaedics, Alpert Medical School of Brown University, Providence, RI 02903 USA

Yuanyuan Zhang

Wake Forest Institute for Regenerative Medicine, Winston-Salem, NC 27157 USA

Abstract

Human urine-derived stem cells (hUSCs) are a newly found stem cell with a potential for therapeutic application in urology. The aim of this study was to investigate whether hUSCs contributed to cartilage regeneration. Despite the characterization with multi-lineage differentiation capacities, in terms of osteogenesis, adipogenesis, and myogenesis, hUSCs did not show the ability to differentiate into chondrocytes. Human bone marrow stromal cells (hBMSCs) are a tissue-specific stem cell for endochondral bone formation; however, repeated passage hBMSCs have less capacity for chondrogenic differentiation. Our findings showed that

Corresponding author: Ming Pei MD, PhD, Stem Cell and Tissue Engineering Laboratory, Department of Orthopaedics, West Virginia University, PO Box 9196, One Medical Center Drive, Morgantown, WV 26506-9196, USA, Telephone: 304-293-1072; Fax: 304-293-7070; mpei@hsc.wvu.edu.

extracellular matrix deposited by hUSCs (UECM) could greatly recharge repeated passage hBMSCs toward chondrogenic differentiation, which might be explained by trophic factors released by hUSCs that were immobilized in UECM. We also found that ECM from repeated passage hBMSCs (BECM) had a limited rejuvenation effect; the Wnt11-mediated noncanonical signaling pathway might be responsible for UECM-mediated hBMSC rejuvenation and subsequent chondrogenic differentiation. Our data indicated that commercially available UECM from young and healthy donors might provide a simple and promising approach for autologous hBMSC rejuvenation. This study also provides an excellent model to investigate the effect of trophic factors released by stem cells on tissue regeneration without interference by stem cell differentiation.

Keywords

Decellularized stem cell matrix; Monolayer expansion; Urine-derived stem cell; Bone marrow stromal cell; Endochondral bone formation

Introduction

Cell therapy-based bone tissue engineering is a promising biological treatment for large bone defects. There is increasing evidence showing that engineering of hypertrophic cartilage templates as bone substitute materials is a novel approach for bone regeneration via endochondral ossification, an *in vitro* imitation of the embryonic developmental pathway of long bones and the axial skeleton (Kronenberg 2003). Autologous bone regeneration can avoid immune rejection and disease transmission. It is critical to identify an appropriate adult stem cell that is capable not only of chondrogenic differentiation but also of ending in hypertrophy. Under chondrogenic induction, synovium-derived stem cells (SDSCs), a tissue-specific stem cell type for chondrogenesis, have a reduced tendency to become hypertrophic (Jones and Pei 2012; Pei et al. 2008a & b); in contrast, bone marrow stromal cells (BMSCs) showed not only chondrogenic potential but also a 5- to 10-fold increase in osteocalcin and alkaline phosphatase (ALP) (Djouad et al. 2005), indicating that BMSCs are a tissue-specific stem cell for endochondral bone formation (Pei et al. 2011a).

Finding an appropriate stem cell for a tissue-specific lineage differentiation is the first step for successful lineage-specific tissue regeneration. Due to the limited colony-forming potential of nucleated cells in BMSCs (1 in 1,000 – 10,000) (Jo et al. 2007), a large scale cell expansion is needed; however, conventional cell expansion (monolayer culture) results in cell senescence in terms of a loss of cell proliferation and differentiation capacity (Li and Pei 2012a). Our previous findings suggested that decellularized stem cell matrix (DSCM or ECM) is an excellent cell expansion system for stem cell rejuvenation in cartilage engineering and regeneration (Pei et al. 2011b). Despite the fact that early-passage human BMSCs (hBMSCs) could be rejuvenated when expanded on their own ECM (Pei et al. 2011a), our preliminary data showed that repeated passage stem cells might not be rejuvenated by ECM deposited by such senescent stem cells.

Recently, a subpopulation of cells isolated from urine, termed urine-derived stem cells (USCs), was found to possess biological characteristics similar to mesenchymal stem cells

(MSCs), i.e. clonogenicity, cell growth patterns, expansion capacity, multi-lineage differentiation capacity, pro-angiogenic paracrine effects, and immunomodulatory properties (Liu et al. 2013; Zhang et al. 2008). Since human USCs (hUSCs) can be collected using a simple, safe, low-cost, and non-invasive procedure, this stem cell from young and healthy donors can be used as a potential cell source for the preparation of commercially available ECM. In this study, we were curious about whether hUSCs could be a potential stem cell source for cartilage regeneration; we also wondered whether ECM deposited by hUSCs could provide an immobilized trophic stimulation for late-passage hBMSC rejuvenation. Considering that Wnt signaling is a critical pathway in the regulation of chondrogenesis and cartilage development (Yates et al. 2005), we assessed the change in Wnt signals in the ECM-mediated hBMSC chondrogenic differentiation.

Materials and Methods

Cell Culture

Human BMSCs were purchased from Lonza Group Ltd. (Basel, Switzerland) and pooled from five donors (20–43 years old, average 25 years old; three males and two females), as described in our previous study (Pei et al. 2011a). Human USCs were donated by Wake Forest University and approved for this study by the Institutional Review Board. The isolation of hUSCs was described in a previous study (Zhang et al. 2008). Briefly, urine samples were collected from four healthy male individuals. Each urine sample was centrifuged at 500 g for 5 min to collect cells. Both BMSCs and USCs were cultured in growth medium [alpha minimum essential medium (αMEM, Invitrogen, Carlsbad, CA) containing 10% fetal bovine serum (FBS), 100 U/mL penicillin, 100 μg/mL streptomycin, and 0.25 μg/mL fungizone].

USC Characterization

Population doublings (PD) and doubling time (DT)—Human USC cell number and culture time were counted at each passage from passage 0 onwards. PD and DT were calculated using the following formula: $PD=\ln(N_f/N_i)/\ln(2)$; $DT=C_t/PD$ (N_f: final number of cells, N_i: initial number of cells, C_t: culture time)

Flow Cytometry Analysis—Human USCs at passage 2 were stained with specific anti-human antibodies labeled with CD14-APC, CD24-FITC, CD29-PE, CD31-FITC, CD34-APC, CD44-PE, CD45-APC, CD73-APC, CD90-APC, CD105-PE, CD117-PE, CD133-PE, CD146-PE, SSEA-4-PE, and STRO-1-FITC (Table 1). Briefly, trypsinized hUSCs (5×10^5) were re-suspended in ice-cold phosphate buffered saline (PBS) containing 1% bovine serum albumin (BSA). Fluorochrome-conjugated antibodies were added to cells in 50 μL of PBS containing 3% BSA and incubated on ice for 30 min in the dark. IgG1-PE, IgG1-FITC, and IgG1-APC conjugated isotype control antibodies were used to subtract background fluorescence. After filtering through a 70 μm cell strainer, cells were analyzed using flow cytometry (FACS Calibur, BD Biosciences, Franklin Lakes, NJ) and FlowJo software (TreeStar, Inc., Ashland, OR).

Enzyme-linked Immunosorbent Assay (ELISA) Plate Array—A total of 2×10^5 hUSCs at passage 2 were seeded in a six-well plate and then incubated with serum-free αMEM at 37°C in 5% CO_2 for 24 h. The conditioned medium was collected and analyzed by human cytokine ELISA plate array (Signosis, Inc., Sunnyvale, CA) according to the manufacturer's instructions. Briefly, 100 μL of culture supernatants were incubated in 96-well plates on a rocking platform at room temperature for 1 h. After incubating with detection antibody mixture, the plates were measured with chemiluminescent substrate by a luminometer plate reader for relative light unit (RLU).

Multi-lineage Differentiation

<u>**Osteogenic Induction:**</u> hUSCs were seeded at a density of 4000 cells/cm^2 and incubated in an osteogenic induction medium containing low-glucose Dulbecco's Modified Eagle's Medium (DMEM) with 100 nM dexamethasone, 10 mM β-glycerophosphate, and 50 mM ascorbic acid-2-phosphate (Wako Chemicals, Richmond, VA) for 28 days. Osteogenic differentiation was assessed using Alizarin Red S staining (ARS) as described previously (Pei et al. 2011a; Li et al. 2012b).

<u>**Adipogenic Induction:**</u> hUSCs were seeded at a density of 4000 cells/cm^2 and cultured in an adipogenic induction medium containing low-glucose DMEM with 1 μM dexamethasone, 500 μM 3-isobutyl-1-methylxanthine, 10 μg/mL insulin, and 100 μM indomethacin for 28 days. Adipogenic differentiation was assessed using Oil Red O staining (ORO) as described previously (Pei et al. 2011a; Li et al. 2012b).

<u>**Smooth Muscle Cell Induction:**</u> hUSCs were plated at 2000 cells/cm^2 in smooth muscle differentiation media containing equal amounts of high-glucose DMEM and embryonic fibroblast medium (EFM) with 10% FBS, 2.5 ng/mL of transforming growth factor beta1 (TGF-β1), and 5 ng/mL of platelet-derived growth factor BB (PDGF-BB) (R&D Systems, Minneapolis, MN). Cell morphology was recorded before and after growth factor additions for up to 14 days. The slides were fixed with freshly prepared 4% paraformaldehyde for 20 min followed by permeabilization with 0.1% Triton-X100 in PBS for 10 min and blocked with serum-free block solution (Dako, Denmark) for 15 min. Lineage-specific primary antibodies, rabbit polyclonal antibodies to desmin (abcam, Cambridge, MA; catalog number ab15200) and MyoD (C-20, Santa Cruz Biotechnology, Inc., Dallas, TX; catalog number sc-304), were incubated at 4°C overnight followed by secondary antibody conjugated to Alexa Fluor 594 (Life Technologies, Grand Island, NY; catalog number A11072) for 30 min in the dark. The slides were mounted using anti-fade mounting media (Vector Laboratories, Inc., Burlingame, CA) containing propidium iodide (PI) and images were captured using a Leica upright microscope (DM 4000B, Wetzlar, Germany).

ECM Preparation

Passage 3 hUSCs and passage 8 hBMSCs were used to prepare extracellular matrix, UECM and BECM, respectively, as described in our previous study (Pei et al. 2011a; He et al. 2009). Briefly, when the cells seeded on plastic flasks (Plastic) reached 90% confluence, 50 μM of L-ascorbic acid phosphate (Wako Chemicals USA, Inc.) was added for 8 days. The deposited matrix was incubated with 0.5% Triton X-100 containing 20 mM ammonium

hydroxide at 37°C for 5 min and stored at 4°C in PBS containing 100 U/mL penicillin, 100 μg/mL streptomycin, and 0.25 μg/mL fungizone.

Human USC-derived ECM Characterization

Scanning Electronic Microscopy (SEM)—Representative samples (n=2) were primarily fixed in 2.5% glutaraldehyde for 2 h followed by secondary fixation in 2% osmium tetroxide as described previously (Tan et al. 2010). The samples were then dehydrated consecutively in 25%, 50%, 75%, 95%, and 100% ethanol for 10 min each, in hexamethyldisilazane (HMDS) at a ratio of 1:1 with ethanol twice for 1 h each time, in HMDS at a ratio of 1:2 with ethanol overnight, and in HMDS three times for 4 h each time. The samples were air-dried for 24 h and gold sputter was added. The images were recorded by an SEM (Model S 2400; Hitachi, Brisbane, CA).

Immunofluorescent Staining—ECM was fixed with 4% paraformaldehyde in PBS for 30 min. After incubation in 10% normal goat serum for 1 h, ECM was treated with mouse monoclonal antibodies to type I collagen (Clone COL1, Sigma-Aldrich, St. Louis, MO, catalog number C2456), fibronectin (EP5, Santa Cruz Biotechnology, Inc., catalog number sc-8422), and laminin 5 (P3E4, Santa Cruz Biotechnology, Inc., catalog number sc-13587) at 4°C overnight, followed by incubation in Alexa Fluor 488 goat anti-mouse IgG (Life Technologies) for 30 min.

Expanded Cell Chondrogenic Induction and Evaluation

Passage 3 hUSCs and passage 8 hBMSCs were expanded on Plastic, UECM, or BECM for one passage. Upon reaching confluence, the expanded cells (3×10^5 cells) were centrifuged to form a pellet. After overnight incubation (day 0), the pellets were cultured in a serum-free chondrogenic medium consisting of high-glucose DMEM, 40 μg/mL proline, 100 nM dexamethasone, 100 U/mL penicillin, 100 μg/mL streptomycin, 0.1 mM ascorbic acid-2-phosphate, and 1×ITS™ Premix (BD Biosciences) with supplementation of 10 ng/mL TGF-β3 (PeproTech Inc., Rocky Hill, NJ) in a 5% O_2 and 5% CO_2 incubator for 14 days.

Histology and Immunostaining—The pellets (n=3) were fixed in 4% paraformaldehyde at 4°C overnight, followed by dehydrating in a gradient ethanol series, clearing with xylene, and embedding in paraffin blocks. Five-μm sections were stained with Alcian blue (counterstained with fast red) for sulfated glycosaminoglycans (GAGs). The sections were also immunolabeled with primary antibodies against type II collagen (Developmental Studies Hybridoma Bank, Iowa City, IA; catalog number II-II6B3) and type X collagen (Sigma-Aldrich, catalog number C7974), followed by the secondary antibody of biotinylated horse anti-mouse IgG (Vector Laboratories, Inc.). Immunoactivity was detected using Vectastain ABC reagent (Vector Laboratories, Inc.) with 3,3′-diaminobenzidine as a substrate.

Biochemical Analysis—The pellets (n=4) were digested at 60°C for 4 h with 125 μg/mL papain in PBE buffer (100 mM phosphate and 10 mM ethylenediaminetetraacetic acid, pH 6.5) containing 10 mM cysteine. The amount of DNA in the papain digestion was measured using the QuantiT™ PicoGreen® dsDNA assay kit (Invitrogen) with a CytoFluor® Series

4000 (Applied Biosystems, Foster City, CA). GAG was measured using dimethylmethylene blue dye and a Spectronic BioMate 3 Spectrophotometer (Thermo Scientific, Milford, MA) with bovine chondroitin sulfate as a standard.

TaqMan® Real-Time Polymerase Chain Reaction (PCR)—Total RNA was extracted from samples (n=4) using an RNase-free pestle in TRIzol® (Invitrogen). About 1 μg of mRNA was used for reverse transcriptase with a High-Capacity cDNA Archive Kit (Applied Biosystems) at 37°C for 120 min. Chondrogenic marker genes [type II collagen (*COL2A1*) and aggrecan (*ACAN*)] and a hypertrophic marker gene [type X collagen (*COL10A1*)] were customized by Applied Biosystems as part of the Custom TaqMan® Gene Expression Assays (Pei et al. 2013). Eukaryotic 18S RNA (Assay ID HS99999901_s1) was carried out as the endogenous control gene. Real-time PCR was performed with the iCycler iQ™ Multi-Color Real Time PCR Detection (Perkin-Elmer, Waltham, MA). Relative transcript levels were calculated as $\chi=2^{-\Delta\Delta Ct}$, in which $\Delta\Delta Ct = \Delta E - \Delta C$, $\Delta E = Ct_{exp} - Ct_{18s}$, and $\Delta C = Ct_{ct1} - Ct_{18s}$.

Western Blot—To further determine potential mechanisms underlying ECM-mediated cell chondrogenic differentiation, the pellets from expanded hBMSCs were homogenized on dry ice and dissolved in lysis buffer (Cell Signaling, Danvers, MA) with protease inhibitors. Total proteins were quantified using the BCA™ Protein Assay Kit (Thermo Fisher Scientific, Waltham, MA). Thirty micrograms of protein from each sample were denatured and separated using NuPAGE® Novex® Bis-Tris Mini Gels (Invitrogen) in the XCell SureLock™ Mini-Cell (Invitrogen) at 120 V at 4°C for 3 h. Bands were transferred onto a nitrocellulose membrane (Invitrogen) using an XCell II™ Blot Module (Invitrogen) at 15 V at 4°C overnight. The membrane was incubated with primary monoclonal antibodies in 5% BSA, 1×TBS (10 mM Tris-HCl, 150 mM NaCl, pH 7.5), and 0.05% Tween-20 at room temperature for 1 h (β-actin served as an internal control), followed by the secondary antibody of horseradish peroxidase–conjugated goat anti-mouse (Thermo Fisher Scientific) for 1 h. SuperSignal West Femto Maximum Sensitivity Substrate (Thermo Fisher Scientific) and CL-XPosure Film (Thermo Fisher Scientific) were used for exposure. The primary antibodies used in immunoblotting included the Wnt3a (C64F2) monoclonal antibody (Cell Signaling, catalog number 2721), Wnt5a monoclonal antibody (Cell Signaling, catalog number 2530), and Wnt11 polyclonal antibody (Thermo Fisher Scientific, catalog number PIPA521712).

Statistical Analysis

Numerical data are presented as the mean and the standard error of the mean. The Mann-Whitney U test was used for pair-wise comparison in biochemistry and real-time PCR data analysis. All statistical analyses were performed with SPSS 13.0 statistical software (SPSS Inc., Chicago, IL). *P* values less than 0.05 were considered statistically significant.

Results

Characterization of hUSCs

To determine whether hUSCs exhibited MSC surface phenotypes, flow cytometry data showed that hUSCs were strongly positive for typical MSC markers, such as CD24 (heat stable antigen, HSA), CD29 (integrin β1), CD44 (hyaluronan receptor), CD73 (SH3/4), CD90 (Thy-1), CD146 (melanoma cell adhesion molecule, MCAM), and SSEA-4 (stage-specific embryonic antigen 4) (Fig. 1ai). CD105 (SH2 and endoglin), CD133 (prominin 1), and STRO-1 (Fig. 1aii) were weak; and monocyte/macrophage markers such as CD14 and endothelial markers such as CD31 (platelet endothelial cell adhesion molecule, PECAM-1) as well as hematopoietic stem cell markers such as CD34 and CD45 (Fig. 1aiii) were negative.

To evaluate whether hUSCs had MSC proliferation capacity, we measured hUSC population doublings (PD) and doubling times (DT). Our data indicated that the average PD from passage 0 forward to passage 8 of hUSCs was 61.97 ± 4.80 and the average DT was 27.02 ± 12.82 h. To determine whether hUSCs had multi-lineage differentiation potentials, hUSCs were incubated in either osteogenic or adipogenic induction medium for 28 days. Osteogenically differentiated hUSCs appeared to produce mineralized tissue demonstrated by Alizarin Red S staining for calcium deposition (Fig. 1b). Adipogenically differentiated hUSCs were positive for Oil Red O staining (Fig. 1c). Additionally, when hUSCs were cultured in myogenic differentiation medium for 14 days, they became elongated and spindle-shaped; immunostaining by desmin (Fig. 1d) and nuclear staining with antibodies to MyoD (Fig. 1e) revealed the myogenic differentiated populations.

To determine whether the supernatant of hUSCs contained trophic factors, a human cytokine ELISA plate array was used to measure the abundance of 31 human cytokines simultaneously (Fig. 1f). Our data suggested that the cytokines secreted by hUSCs included Adipo (adipokines), b-FGF (basic fibroblast growth factor), b-NGF (beta-nerve growth factor), EGF (epidermal growth factor), G-CSF (granulocyte colony-stimulating factor), GM-CSF (granulocyte/macrophage colony-stimulating factor), IFNγ (interferon-gamma), IL-1α (interleukin-1 alpha), IL-2, IL-4, IL-8 (CXCL8), IL-10, IL-12, IL-13, IP-10 (gamma-interferon inducible protein 10, CXCL10), Leptin, MCP-1 (monocyte chemoattractant protein 1, CCL2), MIP-1α (macrophage inflammatory protein-1 alpha, CCL3), PAI-1 (plasminogen activator inhibitor-1), PDGF-BB, PLGF (placenta growth factor-1), Resistin, TGF-b, TNFα (tumor necrosis factor alpha), and VEGF (vascular endothelial growth factor); the undetectable factors included Eotaxin-3 (CCL26), IGF-I (insulin-like growth factor I), IL-6, IL-17a, Rantes (CCL5), and SCF (stem cell factor).

Physicochemical Properties of UECM

To observe the morphology of UECM, hUSCs were used to secrete matrix followed by chemical treatment to remove hUSCs. SEM data showed that UECM consisted of matrix fibers and inter holes (Fig. 2a); hBMSCs grown on UECM exhibited a fibroblast-like shape (Fig. 2b). To determine the chemical composition of UECM, immunostaining was used to detect three main matrix proteins: collagen, fibronectin, and laminin. Our data clearly

showed that UECM fibers consisted of type I collagen (Fig. 2c) and fibronectin (Fig. 2d) rather than laminin 5 (Fig. 2e).

hUSCs Are Not an Appropriate Stem Cell Source for Chondrogenesis

Compared to the fibroblast-like shape of hBMSCs (Fig. 2f–h), hUSCs exhibited a glistening cobblestone appearance (Fig. 2i-k). When expanded cells were chondrogenically induced, hUSC pellets from both UECM (UonU) and BECM (UonB) expansion gradually became tiny and then disappeared. Compared to those from hBMSCs expanded on corresponding substrates [on Plastic (BonP) (Fig. 3b,f), on BECM (BonB) (Fig. 3c,g), and on UECM (BonU) (Fig. 3d,h)], the pellets from hUSCs expanded on Plastic (UonP) were the smallest in size (Fig. 3a,e) with non-detectable chondrogenic expression at either the protein level (Fig. 3a–d: sulfated GAGs and Fig. 3e–h: type II collagen; Figure 3j: ratio of GAG to DNA) or the mRNA level (Fig. 3k: *ACAN* and Fig. 3l: *COL2A1*) despite surviving a 14-day chondrogenic induction.

ECM Deposited by Repeated Passage hBMSCs Had Decreased Rejuvenation Ability

Despite no evident difference in chondrogenic differentiation markers of expanded cells on either BECM (Fig. 3c,g) or Plastic (Fig. 3b,f), biochemical analysis data suggested that hBMSCs expanded on Plastic (BonP) yielded pellets with a lower GAG amount compared with those grown on BECM (BonB) (data not shown); even though hBMSCs grown on BECM (BonB) yielded pellets with a higher cell viability (DNA ratio adjusted by day 0) (Fig. 3i), there was not a significant difference in chondrogenic index (GAG/DNA) of hBMSC pellets from Plastic (BonP) and BECM (BonB) expansion (Fig. 3j). Despite the fact that hBMSCs grown on BECM yielded pellets with higher *ACAN* (Fig. 3k) and *COL2A1* (Fig. 3l) compared with those plated on Plastic, our hypertrophy data suggested that there was no significant difference in type X collagen immunostaining (Fig. 4a–d) and *COL10A1* mRNA level (Fig. 4e), indicating that BECM expansion in this study had less rejuvenation effect on hBMSC endochondral ossification compared to a previous study (Pei et al. 2011a); replicative senescence from ECM deposited cells was possibly a major factor.

ECM Deposited by hUSCs Preconditioned hBMSCs for Chondrogenic Hypertrophy

Surprisingly, passage 8 hBMSCs expanded on UECM exhibited a strongly enhanced chondrogenic potential, as evidenced by an impressively large pellet size with intensified staining of sulfated GAGs (Fig. 3d) and type II collagen (Fig. 3h). These results were supported by biochemical data in which hBMSCs expanded on UECM (BonU) yielded pellets with the highest GAG amount and chondrogenic index (Fig. 3j) and real-time PCR data in which hBMSCs grown on UECM (BonU) yielded pellets with the highest mRNA levels of *ACAN* (Fig. 3k) and *COL2A1* (Fig. 3l). Interestingly, chondrogenic hypertrophy was concomitantly promoted, as evidenced by immunostaining for type X collagen (Fig. 4a-d) and real-time PCR for *COL10A1* mRNA (Fig. 4e). The above data indicate that expansion on UECM strengthens repeated passage hBMSCs' chondrogenic capacity.

Involvement of Wnt11-mediated Noncanonical Signaling Pathway in the Rejuvenation of hBMSCs by UECM

To determine whether the Wnt signals were regulated during the chondrogenic differentiation of hBMSCs after expansion on different substrates, western blot was used to detect Wnt3a (a typical activator for canonical Wnt signaling), Wnt5a, and Wnt11 (both are typical activators for noncanonical Wnt signaling) in hBMSC pellets at day 0 (24 h after forming a pellet but before chondrogenic induction), day 7 (early stage of chondrogenic induction), and day 14 (late stage of chondrogenic induction). Our data suggested that, under chondrogenic induction, both Wnt3a (Fig. 5a) and Wnt5a (Fig. 5b) increased their expression in hBMSC pellets, especially in those from BECM expansion. In contrast, hBMSCs grown on UECM yielded pellets with an enhanced expression of Wnt11 (Fig. 5c) during chondrogenic induction compared with a decline in the groups preconditioned on either Plastic or BECM, possibly indicating the active involvement of Wnt11 in UECM preconditioned hBMSC chondrogenic differentiation.

Discussion

Urine-derived stem cells were first reported in 2008 and had the ability to differentiate into cell lineages expressing urothelial, smooth muscle, endothelial, and interstitial cell markers, therefore providing a potential cell source for urological tissue reconstruction (Zhang et al. 2008). In this study, we wanted to determine whether hUSCs could differentiate into mesenchymal tissues, especially cartilage; we also wondered whether ECM deposited by hUSCs could contribute to stem cell chondrogenic differentiation. For the first time, we demonstrated that hUSCs were not able to differentiate into chondrocytes despite the fact that hUSCs could differentiate into osteocytes, adipocytes, and myocytes. ECM deposited by hUSCs could recharge senescent hBMSCs toward chondrogenic differentiation; ECM deposited by repeated passage hBMSCs had a limited rejuvenation effect on expanded cells. The Wnt11-mediated noncanonical signaling pathway might be responsible for hUSC-deposited ECM-mediated hBMSC rejuvenation in terms of chondrogenic potential (see summary flowchart in Fig. 6).

It is well-known that senescence-related issues prevent expanded cells from being clinically useful (Li et al. 2012a). Our previous study showed that passage 5 hBMSCs could be rejuvenated after expansion on ECM deposited by passage 5 hBMSCs (Pei et al. 2011a). In this study, we found that passage 8 hBMSCs could not be rejuvenated after expansion on ECM deposited by passage 8 hBMSCs. This finding suggested that replicative senescence might be the reason that hBMSCs lose their differentiation capacity (Vacanti et al. 2005) and ECM loses its "stem cell cue" signals. Intriguingly, passage 8 hBMSCs could be rejuvenated after expansion on ECM deposited by hUSCs, which is superior in chondrogenic capacity to passage 5 hBMSCs after expansion on ECM deposited by hBMSCs (Pei et al. 2011a), as evidenced by the ratio of GAG to DNA after 7-day-chondrogenic induction (5.98 ± 0.34 versus 3.62 ± 0.80, $p=0.0032$), while hUSCs did not show any ability for differentiation into chondrocytes even after expansion on ECM from either stem cell type, indicating that trophic effects from ECM deposited by hUSCs might play a key role in rejuvenating senescent hBMSC chondrogenic potential. Type X collagen was concomitantly up-regulated

at both the protein and mRNA levels in chondrogenically differentiated hBMSCs after expansion on ECM deposited by hUSCs, reminiscent of hBMSCs as a tissue-specific stem cell for endochondral ossification (Jones and Pei 2012; Pei et al. 2011a; Shen 2005).

By using human cytokine ELISA plate array, we were able to detect the trophic factors released by hUSCs. The trophic factors detected in this study included various kinds of growth, inflammatory, and immunomodulatory factors. In the growth factor category, the first ones deserving attention are VEGF-related factors consisting of VEGF, PLGF, and PDGF. The formation of new vasculature is critical to regeneration and repair as both the driver and orientor of new bone formation. In this context, MSCs are proposed to be largely derived from pericytes associated with vasculature. A comprehensive perspective is presented in which signaling molecules such as PDGF take on new significance in vasculature-pericyte-MSC-osteoblast dynamics. Current data suggest that PDGF could function as a central connector between the cellular components and contributors of the osteoblast differentiation program. The inference is that PDGF could function at sites of injury to mobilize pericytes, stimulate mitotic expansion of these cells, and help organize them. In this way, PDGF both contributes to the osteogenic lineage and helps to stabilize newly forming vessels that act to drive the multistep, multicomponent cascade of new bone formation (Caplan and Correa 2011). The second in the growth factor category is adipo-related factors, such as Resistin, PAI-1, Leptin, and Adipo. Considering adipose-derived stem cells show a reduced chondrogenic differentiation capacity under standard induction conditions (Sakaguchi et al. 2005; Winter et al. 2003), adipo-related properties might explain why hUSCs in this study had an undetectable chondrogenic capacity. The third one is anabolic growth factors, such as b-FGF, EGF, and TGF-β. The FGFs play a central role during prenatal development and postnatal growth and regeneration of a wide variety of tissues, by promoting cellular proliferation and differentiation. All members of the FGF family bind, with varying degrees of affinity, to heparin sulfate proteoglycans, which serve as an extracellular storage site and, in some cases, appear to be involved in the activation of the FGF receptors. EGF is a potent growth factor that stimulates the proliferation of various epidermal and epithelial cells. TGF-β is a protein that controls proliferation, cellular differentiation, and other functions in most cells. Interestingly, there was no detectable IGF-I and SCF in the released factors from hUSCs. The IGFs are mitogenic polypeptide growth factors that stimulate the proliferation and survival of various cell types including muscle, bone, and cartilage tissue *in vitro*. It is unknown whether the lack of IGF-I release has any relationship with undetectable chondrogenic differentiation in hUSCs.

Immunomodulatory factors include interleukins, such as IL-2 and IL-12, cytokines, such as IFN and G-CSF, and chemokines, such as MIP-1α. IL-2 is a powerful immunoregulatory lymphokine produced by T-cells in response to antigenic or mitogenic stimulation. By inducing IFNγ production by natural killer (NK) and T cells, IL-12 is a potent regulator of cell mediated immune responses. Among its biological activities, IL-12 promotes the growth and activity of activated NK, CD4+, and CD8+ cells and induces the development of IFNγ producing Th1 cells. IFNγ signaling in antigen-presenting cells and antigen-recognizing B and T lymphocytes regulates the antigen-specific phases of the immune response. Additionally, IFNγ stimulates a number of lymphoid cell functions including the anti-

microbial and anti-tumor responses of macrophages, NK cells, and neutrophils. G-CSF, a colony-stimulating factor hormone, is a glycoprotein, growth factor, and cytokine produced by a number of different tissues to stimulate the bone marrow to produce granulocytes and stem cells. MIP is crucial for immune responses to infection and inflammation (Ren et al. 2010).

In our study, hUSCs were not able to differentiate into chondrocytes while immobilized trophic stimulation in the ECM deposited by hUSCs contributed to repeated passage hBMSC chondrogenic potential, suggestive of a paradigm shift that paracrine actions from stem cells may serve as a major beneficial effect in lieu of differentiation. The trophic factors secreted by stem cells can be delivered and exert potential paracrine effects on other cell types through two approaches: soluble trophic factors in culture medium and immobilized trophic factors in ECM. The methods to isolate and concentrate stem cell-conditioned media have been recently reported for harnessing the trophic factors produced by stem cells (Gnecchi and Melo 2009); however, certain limitations exist for the therapeutic use of stem cell-conditioned media, which include concerns about contamination by animal products, the *in vitro* half lives of molecules secreted by stem cells, and the relative amounts of secreted factors and the effective dosage necessary to elicit a functional response *in vivo*. In the ECM remaining. Since matrix contains not only structural elements, such as collagens, laminins, and fibronectin, but also functional elements, such as FGF, PDGF, VEGF, and TGF (Baraniak and McDevitt 2010), the exogenous administration of an ECM may catalyze tissue regeneration through paracrine actions of morphogenic biomolecules sequestered within the matrix.

Since Wnt signaling is actively involved in TGF-β-mediated MSC chondrogenesis, we expected to observe the relationship between chondrogenic potential of expanded hBMSCs after preconditioning and the Wnt signaling pathways. It is well known that Wnt3a is a canonical Wnt protein, signaling through a β-catenin-dependent signaling pathway. Genetic deletion of β-catenin from early osteoprogenitors resulted in a lack of mature osteoblasts in the mouse embryo, whereas forced activation of β-catenin greatly enhanced osteogenesis (Rodda and McMahon 2006). On the contrary, Wnt3a mediated inhibition of chondrogenesis in micromass cultures of embryonic chick limb-bud cells (Surmann-Schmitt et al. 2009); Wnt3a strongly repressed chondrogenesis and chondrocyte gene expression in cultured chondrocytic cells and differentiating limb-bud mesenchyme (Reinhold et al. 2006). In contrast to Wnt3a, Wnt5a and Wnt11 regulate cartilage-specific matrix molecules through the noncanonical pathway. Despite its function in regulating chondrogenesis, limb development, and longitudinal skeletal outgrowth (Kawakami et al. 1999; Yang et al. 2003), forced expression of Wnt5a delays chondrocyte maturation by inhibiting type X collagen expression, a marker for hypertrophic chondrocytes (Tufan and Tuan 2001). Thus both Wnt3a and Wnt5a inhibit cartilage maturation, which might explain our data showing that 14-day chondrogenically differentiated hBMSCs in either the BECM or Plastic expansion group exhibited higher expression of Wnt3a and Wnt5a but lower chondrogenic differentiation. In the case of Wnt11, its expression is restricted to the prehypertrophic chondrocytes of the cartilage elements, but it does not affect chondrogenic differentiation or hypertrophy of chondrocytes in chick micromass culture (Church et al. 2002; Loganathan et

al. 2005). Wnt11 has been demonstrated to be capable of inhibiting canonical Wnt signaling through various intracellular pathways (Maye et al. 2004), which is consistent with our data that 14-day chondrogenically differentiated hBMSCs in the UECM expansion group displayed enhanced chondrogenic differentiation concomitantly with an up-regulation of Wnt11 expression. Our results are corroborated by a recent report that Wnt5a inhibits type II collagen expression by activating the c-Jun N-terminal kinases (JNK) pathway, whereas Wnt11 enhances type II collagen expression by activating the protein kinase C (PKC) signaling pathway. These results suggest that Wnt5a is associated with cartilage destruction, whereas Wnt11 plays a role in the maintenance of cartilage homeostasis (Ryu and Chun 2006).

In conclusion, we found that expansion of matrix deposited by nonchondrogenic USCs strengthened repeated passage hBMSCs's chondrogenic capacity. We believe USCs can be an excellent model for interpretation of stem cell trophic effect because this stem cell itself does not differentiate into chondrocytes but its matrix contributes to other stem cells' chondrogenic capacity. Expansion on UECM was also found to be responsible for the up-regulation of Wnt11 in hBMSCs during the subsequent chondrogenic induction; gain-of-function and loss-of-function strategies will benefit further elucidation of the in-depth role of Wnt signals in ECM-mediated hBMSC rejuvenation. Despite important findings in this study, there are some limitations that deserve further investigation. For example, collagen, fibronectin, and laminin are three major components in extracellular matrix (Dickinson et al. 2011); surprisingly, in the UECM, we detected type I collagen and fibronectin and no laminin 5. As we know, laminins are major proteins in the basal lamina, the protein network foundation for most cells and organs, influencing cell differentiation, migration, and adhesion, as well as phenotype and survival (Timpl et al. 1979). A comprehensive analysis of matrix components, such as proteomics, is needed to uncover the rejuvenation effect of ECM on expanded cells. Despite the focus of this study on whether USCs contributed to cartilage regeneration, the effect of ECM rejuvenation on hBMSC proliferation, apoptosis, senescence, and cell cycle is also important and deserves more attention in future investigations.

Acknowledgments

References

Baraniak PR, McDevitt TC. Stem cell paracrine actions and tissue regeneration. Regen Med. 2010; 5:121–143. [PubMed: 20017699]

Caplan AI, Correa D. PDGF in bone formation and regeneration: new insights into a novel mechanism involving MSCs. J Orthop Res. 2011; 29:1795–1803. [PubMed: 21618276]

Church V, Nohno T, Linker C, Marcelle C, Francis-West P. Wnt regulation of chondrocyte differentiation. J Cell Sci. 2002; 115:4809–4818. [PubMed: 12432069]

Dickinson LE, Kusuma S, Gerecht S. Reconstructing the differentiation niche of embryonic stem cells using biomaterials. Macromol Biosci. 2011; 11:36–49. [PubMed: 20967797]

Djouad F, Bony C, Häupl T, Uzé G, Lahlou N, Louis-Plence P, Apparailly F, Canovas F, Rème T, Sany J, Jorgensen C, Noël D. Transcriptional profiles discriminate bone marrow-derived and synovium-derived mesenchymal stem cells. Arthritis Res Ther. 2005; 7:R1304–R1315. [PubMed: 16277684]

Gnecchi M, Melo LG. Bone marrow-derived mesenchymal stem cells: isolation, expansion, characterization, viral transduction, and production of conditioned medium. Methods Mol Biol. 2009; 482:281–294. [PubMed: 19089363]

He F, Chen XD, Pei M. Reconstruction of an in vitro tissue-specific microenvironment to rejuvenate synovium-derived stem cells for cartilage tissue engineering. Tissue Eng Part A. 2009; 15:3809–3821. [PubMed: 19545204]

Jo CH, Ahn HJ, Kim HJ, Seong S, Lee MC. Surface characterization and chondrogenic differentiation of mesenchymal stromal cells derived from synovium. Cytotherapy. 2007; 9:316–327. [PubMed: 17573607]

Jones B, Pei M. Synovium-derived stem cells: a tissue-specific stem cell for cartilage tissue engineering and regeneration. Tissue Eng Part B Rev. 2012; 18:301–311. [PubMed: 22429320]

Kawakami Y, Wada N, Nishimatsu SI, Ishikawa T, Noji S, Nohno T. Involvement of Wnt-5a in chondrogenic pattern formation in the chick limb bud. Dev Growth Differ. 1999; 41:29–40. [PubMed: 10445500]

Kronenberg HM. Developmental regulation of the growth plate. Nature. 2003; 423:332–336. [PubMed: 12748651]

Li JT, Jones B, Zhang Y, Vinardell T, Pei M. Low density expansion rescues human synovium-derived stem cells from replicative senescence. Drug Deliv Transl Res. 2012b; 2:363–374.

Li JT, Pei M. Cell senescence: a challenge in cartilage engineering and regeneration. Tissue Eng Part B. 2012a; 18:270–287.

Liu G, Pareta RA, Wu R, Shi Y, Zhou X, Liu H, Deng C, Sun X, Atala A, Opara EC, Zhang Y. Skeletal myogenic differentiation of urine-derived stem cells and angiogenesis using microbeads loaded with growth factors. Biomaterials. 2013; 34:1311–1326. [PubMed: 23137393]

Loganathan PG, Nimmagadda S, Huang R, Scaal M, Christ B. Comparative analysis of the expression patterns of Wnts during chick limb development. Histochem Cell Biol. 2005; 123:195–201. [PubMed: 15778857]

Maye P, Zheng J, Li L, Wu D. Multiple mechanisms for Wnt11-mediated repression of the canonical Wnt signaling pathway. J Biol Chem. 2004; 279:24659–24665. [PubMed: 15067007]

Pei M, He F, Kish V, Vunjak-Novakovic G. Engineering of Functional Cartilage Tissue Using Stem Cells from Synovial Lining: A Preliminary Study. Clin Orthop Relat Res. 2008a; 466:1880–1889. [PubMed: 18512111]

Pei M, He F, Kish VL. Expansion on extracellular matrix deposited by human bone marrow stromal cells facilitates stem cell proliferation and tissue-specific lineage potential. Tissue Eng Part A. 2011a; 17:3067–3076. [PubMed: 21740327]

Pei M, He F, Vunjak-Novakovic G. Synovium-derived stem cell-based chondrogenesis. Differentiation. 2008b; 76:1044–1056. [PubMed: 18637024]

Pei M, Li JT, Shoukry M, Zhang Y. A Review of Decellularized Stem Cell Matrix: a Novel Cell Expansion System for Cartilage Tissue Engineering. Eur Cell Mater. 2011b; 22:333–343. [PubMed: 22116651]

Pei M, Zhang Y, Li JT, Chen DQ. Antioxidation of decellularized stem cell matrix promotes human synovium-derived stem cell-based chondrogenesis. Stem Cells Dev. 2013; 22:889–900. [PubMed: 23092115]

Reinhold MI, Kapadia RM, Liao Z, Naski MC. The Wnt-inducible transcription factor Twist1 inhibits chondrogenesis. J Biol Chem. 2006; 281:1381–1388. [PubMed: 16293629]

Ren M, Guo Q, Guo L, Lenz M, Qian F, Koenen RR, Xu H, Schilling AB, Weber C, Ye RD, Dinner AR, Tang WJ. Polymerization of MIP-1 chemokine (CCL3 and CCL4) and clearance of MIP-1 by insulin-degrading enzyme. EMBO J. 2010; 29:3952–3966. [PubMed: 20959807]

Rodda SJ, McMahon AP. Distinct roles for Hedgehog and canonical Wnt signaling in specification, differentiation and maintenance of osteoblast progenitors. Development. 2006; 133:3231–3244. [PubMed: 16854976]

Ryu JH, Chun JS. Opposing roles of WNT-5A and WNT-11 in interleukin-1beta regulation of type II collagen expression in articular chondrocytes. J Biol Chem. 2006; 281:22039–22047. [PubMed: 16754689]

Sakaguchi Y, Sekiya I, Yagishita K, Muneta T. Comparison of human stem cells derived from various mesenchymal tissues: superiority of synovium as a cell source. Arthritis Rheum. 2005; 52:2521–2529. [PubMed: 16052568]

Shen G. The role of type X collagen in facilitating and regulating endochondral ossification of articular cartilage. Orthod Craniofac Res. 2005; 8:11–17. [PubMed: 15667640]

Surmann-Schmitt C, Widmann N, Dietz U, Saeger B, Eitzinger N, Nakamura Y, Rattel M, Latham R, Hartmann C, von der Mark H, Schett G, von der Mark K, Stock M. Wif-1 is expressed at cartilage-mesenchyme interfaces and impedes Wnt3a-mediated inhibition of chondrogenesis. J Cell Sci. 2009; 122:3627–3637. [PubMed: 19755491]

Tan YB, Zhang YY, Pei M. Meniscus reconstruction through co-culturing meniscus cells with synovium-derived stem cells on small intestinal submucosa. Tissue Eng Part A. 2010; 16:67–79. [PubMed: 19619075]

Timpl R, Rohde H, Robey PG, Rennard SI, Foidart JM, Martin GR. Laminin--a glycoprotein from basement membranes. J Biol Chem. 1979; 254:9933–9937. [PubMed: 114518]

Tufan AC, Tuan RS. Wnt regulation of limb mesenchymal chondrogenesis is accompanied by altered N-cadherin-related functions. FASEB J. 2001; 15:1436–1438. [PubMed: 11387249]

Vacanti V, Kong E, Suzuki G, Sato K, Canty JM, Lee T. Phenotypic changes of adult porcine mesenchymal stem cells induced by prolonged passaging in culture. J Cell Physiol. 2005; 205:194–201. [PubMed: 15880640]

Winter A, Breit S, Parsch D, Benz K, Steck E, Hauner H, Weber RM, Ewerbeck V, Richter W. Cartilage-like gene expression in differentiated human stem cell spheroids: a comparison of bone marrow-derived and adipose tissue-derived stromal cells. Arthritis Rheum. 2003; 48:418–429. [PubMed: 12571852]

Yang Y, Topol L, Lee H, Wu J. Wnt5a and Wnt5b exhibit distinct activities in coordinating chondrocyte proliferation and differentiation. Development. 2003; 130:1003–1015. [PubMed: 12538525]

Yates KE, Shortkroff S, Reish RG. Wnt influence on chondrocyte differentiation and cartilage function. DNA Cell Biol. 2005; 24:446–457. [PubMed: 16008513]

Zhang Y, McNeill E, Tian H, Soker S, Andersson KE, Yoo JJ, Atala A. Urine derived cells are a potential source for urological tissue reconstruction. J Urol. 2008; 180:2226–2233. [PubMed: 18804817]
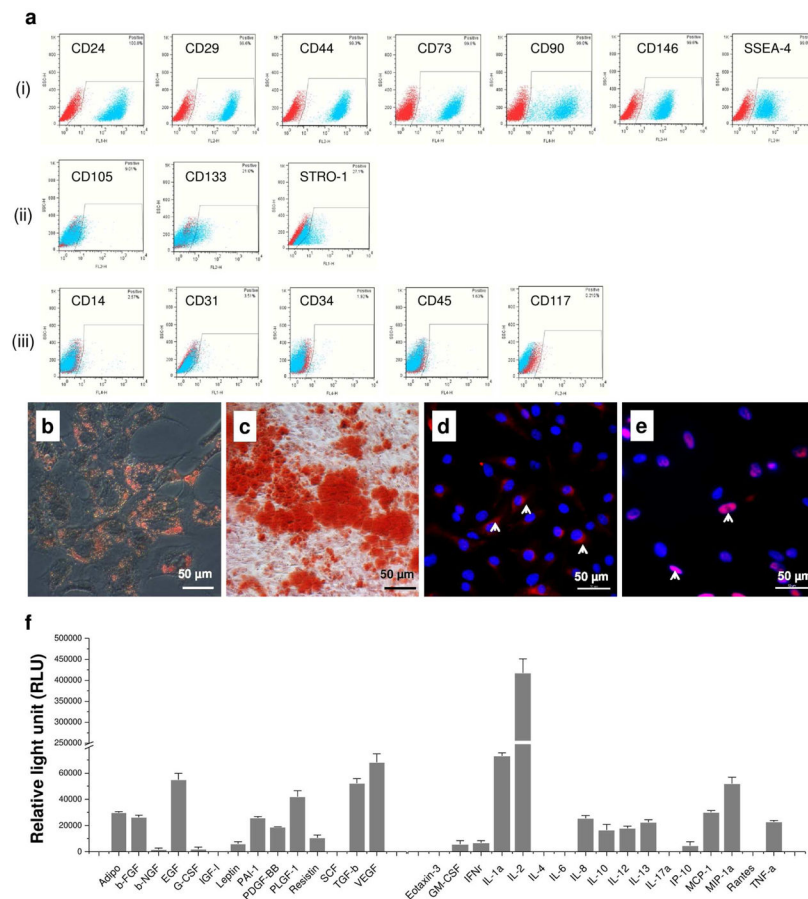
Fig. 1.

Characterization of hUSCs. (**a**) Cell surface marker expression of hUSCs was detected by flow cytometry. Strongly positive markers **i**: CD24, CD29, CD44, CD73, CD90, CD146, and SSEA-4; weakly positive markers **ii**: CD105, CD133, and STRO-1; and negatively expressed markers **iii**: CD14, CD31, CD34, CD45, and CD117. Multi-differentiation potential of hUSCs *in vitro* was evaluated using osteogenic, adipogenic, and myogenic induction. Osteogenic differentiation: (**b**) Alizarin Red S staining for calcium deposition ; adipogenic differentiation: (**c**) Oil Red O staining for lipid droplets ; and myogenic differentiation: immunofluorescent staining (arrows, red) for myogenic marker expression (**d**): Desmin and (**e**): MyoD in induced cells. Scale bar = 50 μm. (**f**) Trophic factors secreted by hUSCs were analyzed by human cytokine ELISA plate array and were mainly categorized as growth factors and immunomodulatory cytokines.
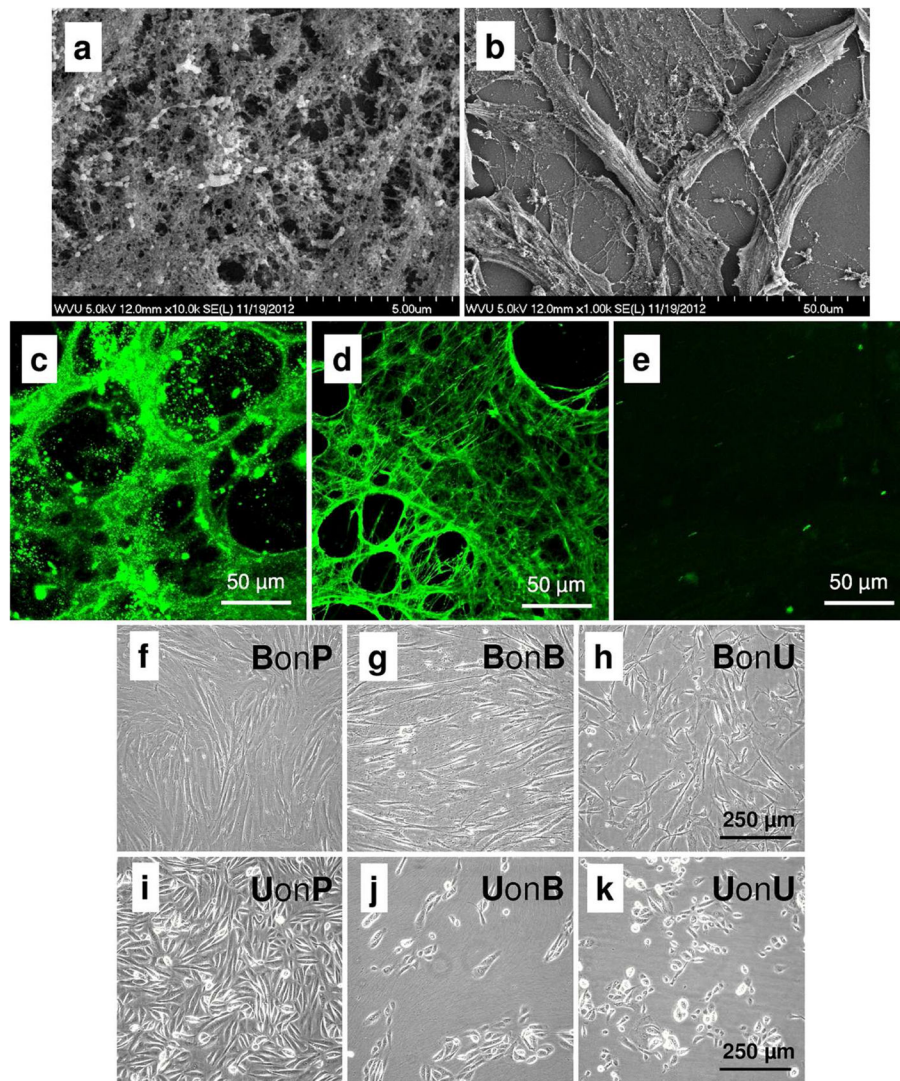
Fig. 2.
UECM physicochemical properties and expanded cell morphology. SEM was used to observe (**a**) UECM (scale bar = 5 μm) and (**b**) hBMSCs grown on UECM (scale bar = 50 μm). Immunofluorescent staining was used to detect (**c**) type I collagen, (**d**) fibronectin, and (**e**) laminin 5. Scale bar = 50 μm. Phase contrast microscope was used to show cell morphology after hBMSCs [(**f**:) BonP, (**g**) BonB, and (**h**) BonU] and hUSCs [(**i**) UonP, (**j**) UonB, and (**k**) UonU] were expanded on Plastic, BECM, and UECM. Scale bar = 250 μm.
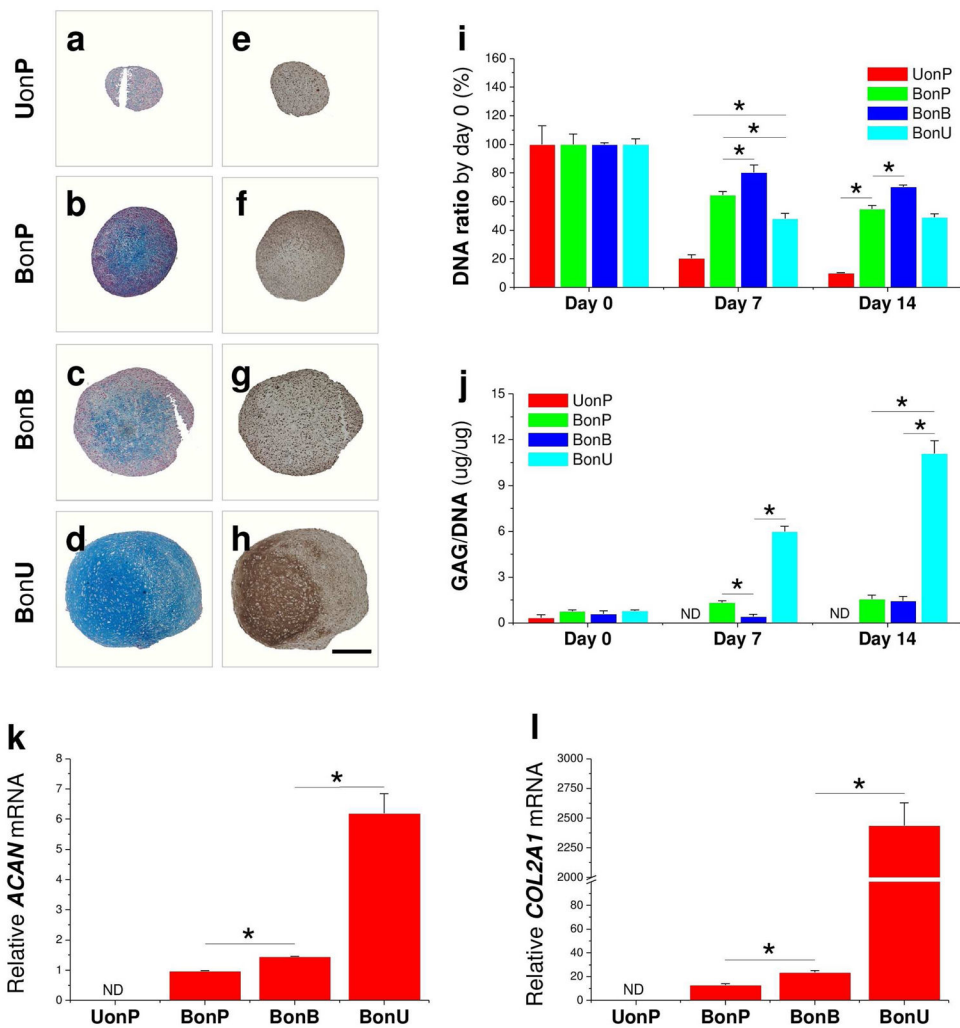
Fig. 3.
Chondrogenic evaluation of expanded cells. After expansion on Plastic, BECM, or UECM, hBMSCs or hUSCs were cultured in a pellet system supplemented with a serum-free chondrogenic medium for 14 days. (**a–d**) Alcian blue staining (AB) and (**e–h**) immunohistochemical staining (IHC) were used to detect sulfated GAGs and type II collagen, respectively. Scale bar = 800 μm. Biochemical analysis was used to measure DNA and GAG amount, which can be used to calculate (**i**) DNA ratio (cell viability) and (**j**) ratio of GAG to DNA (chondrogenic index). TaqMan® real-time PCR was used to evaluate (**k**) *ACAN* and (**l**) *COL2A1* mRNAs. * $p < 0.05$. Data are shown as average ± SD for n = 4.
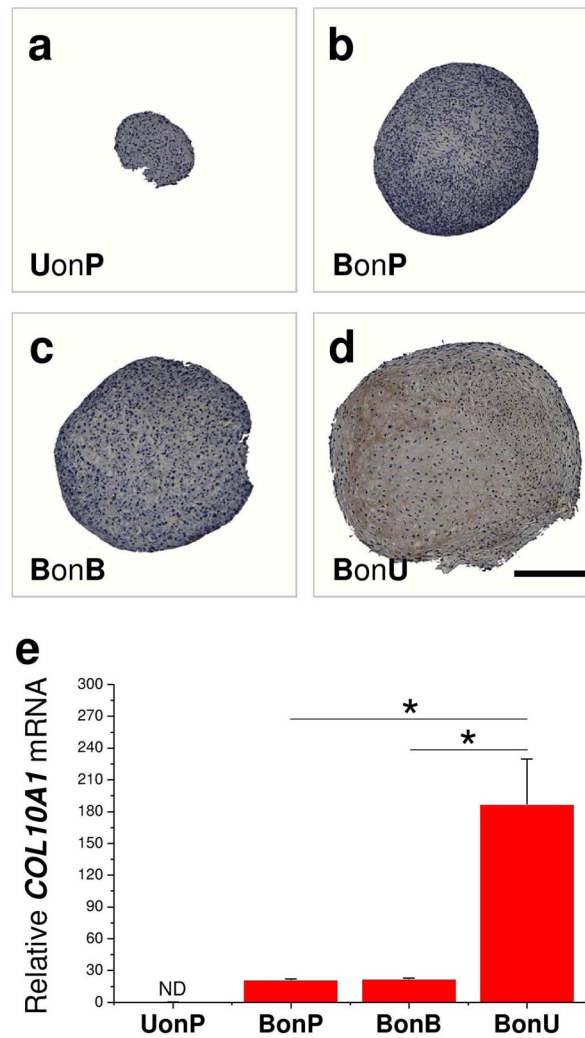
Fig. 4.
Hypertrophic evaluation of expanded cells. After expansion on Plastic, BECM, or UECM, hBMSCs or hUSCs were cultured in a pellet system supplemented with a serum-free chondrogenic medium for 14 days. (**a–d**) Immunohistochemical staining (IHC) was used to detect type X collagen. Scale bar = 800 μm. (**e**) TaqMan® real-time PCR was used to evaluate *COL10A1* mRNA. * $p < 0.05$. Data are shown as average ± SD for n = 4.
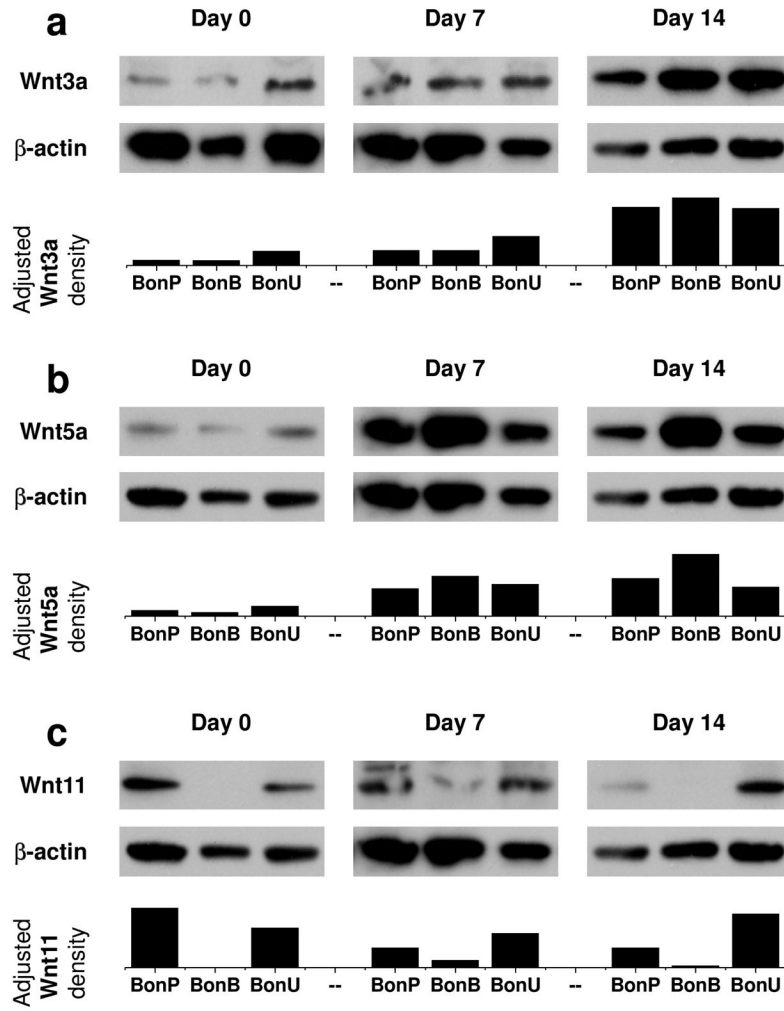
Fig. 5.
Involvement of noncanonical Wnt signaling pathway during chondrogenic induction. The pellets from hBMSCs expanded on three substrates were used to extract proteins for gel running and western blot. The pellets from hUSCs after expansion on Plastic were too tiny to provide sufficient protein for this measurement. Canonical [(**a**) Wnt3a] and noncanonical Wnt [(**b**) Wnt5a and (**c**) Wnt11] signaling pathways were evaluated in chondrogenically differentiated hBMSCs at day 0 (condensation phase), day 7 (early phase of chondrogenic induction), and day 14 (late phase of chondrogenic induction). β-actin served as an internal control. Image J software was used to semi-quantify immunoblotting bands.
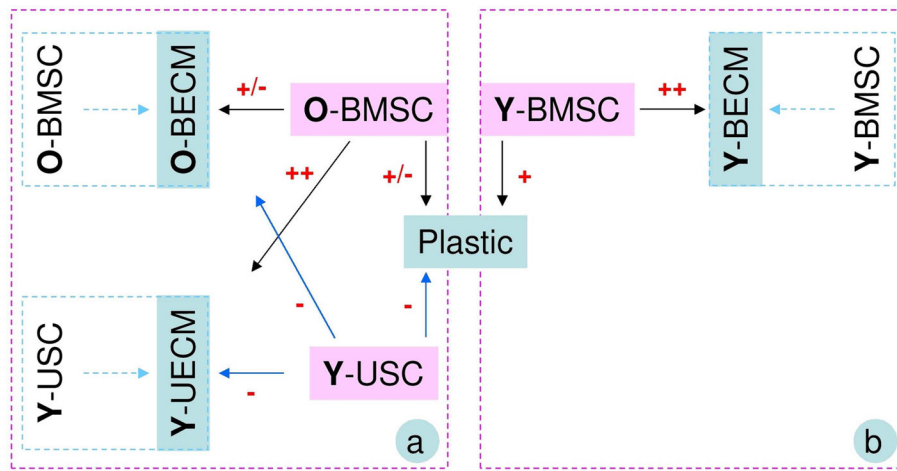
Fig. 6.
A flow chart of the comparison (**a**) between Young UECM (Y-UECM) and Old BECM (O-BECM) from this study and the comparison (**b**) between O-BECM and young BECM (Y-BECM) from a previous study [6]. Chondrogenic potential in either hBMSCs or hUSCs after expansion on Plastic, BECM, or UECM was graded as strongly positive (+++), very positive (++), positive (+), positive/negative (+/−), and negative (−).

Table 1

Detailed information about antibodies used in flow cytometry analysis.

Antibodies	source Ig	against	Company Cat.NO.
CD14-APC	mouse IgG1	Human	R&D system FAB3832A
CD24-FITC	Mouse IgG2a, κ	Human	BD 560992
CD29-PE	Mouse IgG1, κ	Human	BD 555443
CD29-PE	Mouse IgG2a, κ	Human	BD 556049
CD31-FITC	Mouse IgG1, κ	Human	BD 560984
CD34-FITC	Mouse IgG	Human	BD 348053
CD44-PE	Mouse IgG1, κ	Human	BD 550989
CD45-APC	Mouse IgG1	Human	BD 340943
CD73-PE	Mouse IgG1, κ	Human	BD 550257
CD90-APC	Mouse IgG1, κ	Human	BD 559869
CD105-PE	Mouse IgG1, κ	Human	BD 560839
CD117-PE	mouse IgG 1	Human	BD 340867
CD133-PE	Mouse IgG1	Human	MACS 130080801
CD146-PE	Mouse IgG1, κ	Human	BD 550315
STRO-FITC	Mouse IgM, 1	Human	Biolegend 340105
SSEA-4-PE	Mouse IgG3, κ	Human	BD 560128
MsIgG1-PE	Mouse IgG1, κ		BD 559320
MsIgG1-FITC	Mouse IgG1, κ		BD 555909
MsIgG1-APC	Mouse IgG1, κ		BD 555751